Wireless Communications Design

Project Report

Project: Wireless Baseband Modulation Generator

Nabeel Nayyar
3-8-2023

Section 1: Abstract/Introduction

This lab aimed to provide hands-on experience with digital modulation techniques, specifically IQ modulation and symbol streaming, and their implementation in hardware using various instruments like an RF signal generator, an arbitrary waveform generator, a spectrum analyzer, and an oscilloscope.

The lab involved building a circuit that takes an MCP4822 SPI Dual DAC and converts the digital input signals from the Tiva C board to analog signals with a range of +/- 0.5V using a TLC072 op-amp. We also wrote software to write voltage pairs to the DAC output and tested basic modulation (PBSK, QPSK, 8PSK, 16QAM). The lab also includes streaming symbols without filtering and with root-raised cosine (RRC) filtering for smoother constellations of the streamed modulated symbols. Where the DAC is connected to the TM4C123GXL board with Pins specified in Section 2.

Section 2: Procedures

For this Lab report, all hypotheses were tested out using the Signal Generators (for parts 1-4) where we created a tone signal which was connected to the IQ inputs of the signal generator and used external IQ modulation (IQ button) to enable modulation. The RF output (when enabled from the RF Signal generator) was connected to the spectrum analyzer which has been discussed in the next section.

Similarly, if testing the modulations generated from the TM4C123GXL board with pinout as shown in Table 2.1 (and the composite circuit with the dual DAC and the Op-Amp) were connected to the RF Signal Generator and from there to the spectrum analyzer and to test constellations we attached the IQ outputs of the composite circuit that we made in the lab to an oscilloscope with the XY mode turned on.

For testing the RAW, DC, SINE, and TONE modes of the composite circuit we again connected the IQ outputs of the composite circuit to the oscilloscope but without XY mode turned on to see the wave in amplitude (volts V) and time domain.

In some specified cases we also set the oscilloscope in the FFT (Fast Fourier Transform) mode to view the frequency spectrum of the modulated signal to understand the behavior of different modulation techniques we implemented in this lab.

TM4C123GXL Board Pin	Pin definition
PA5	MOSI (SSI0Tx) For SPI DAC Write
PA3	~ Chip Select (SSI0Fss) For DAC Write
PA2	SPI Clock pin (SSI0CLK)
PA4	~ LDAC (Load DAC)

Table 2.1 Pinout of the Tiva C Board with circuit peripheral DAC

Section 3: Results and Discussion of the Results

For the starting steps of the lab, where we tried to modulate an external IQ source on the RF Signal generator, we set the arbitrary signal generator at 10 kHz frequency and set the signal type to a sine wave (for the CH 1) and another sine wave with a 90-degree offset (to imitate a cosine wave) to channel 2 with both the channels set at 0.5 $V_{p\text{-}p}$ to the I and Q inputs of the RF signal Generator (CH 1 to I input and CH 2 to the Q input) with the RF signal generator frequency set to 27.1 MHz and power set to -30 dBm. This was then looped from a BNC cable to the spectrum analyzer. After the IQ modulation was turned on and RF output was enabled. We saw a spike of a singular frequency (27.1000 MHz) in the center of the Spectrum analyzer at a span of 100 kHz. We then observed the upper-sideband modulation where the spike in frequency moved to the left by 10 kHz and then for the lower-sideband modulation we saw the signal frequency shift to the right by 10 kHz in frequency.

When attached only the I input (Q left detached) we saw the spectrum analyzer show double-side modulation where there were two big spikes in frequency on both sides from the center spaced 10 kHz on each side (right and left) with a small spike in the center as well. This was observably intuitive because the quadrature component (Q) carries information about the negative frequencies, and when we removed it, we only observed the positive frequency spectrum. which implied that the spectral efficiency is halved when using a single-sideband modulation technique.

Moving to the circuit build. We designed the circuit which was essential as shown in Figure 3.1 (a block diagram of the circuit)

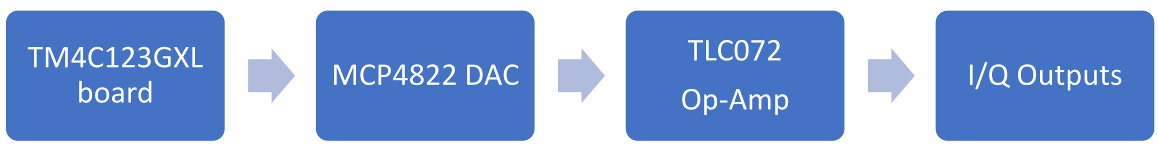

Figure 3.1 Block diagram of the Circuit designed for software-defined modulation.

The Code was written in such a way that there was an interrupt service routine in the Tiva board code (called 'symbolTimerIsr') which was called periodically and updated the DAC values for any modulation or 'signal' to be cast to the I/Q inputs. For the circuit layout, we implemented I output on the Channel A of the DAC and similarly Q output on the Channel B of the DAC chip.

The first implemented mode was to test the generation of Cosine and Sine functions (TONE mode in the code) which was generated by creating a LUT to sequentially write on the DAC when the interrupt service was called. We created the LUT by first calculating the RAW values and their desired voltages from 0 to 4095 and found the points on which the DAC can write voltages from -0.5 V to +0.5 V which have been defined in the source code. The sine and cosine functions were then tested out at 0.5 V amplitude and 10 kHz frequency (very similar to what we did with the arbitrary signal generator above) and had the output waveform as shown in Figure 3.2.

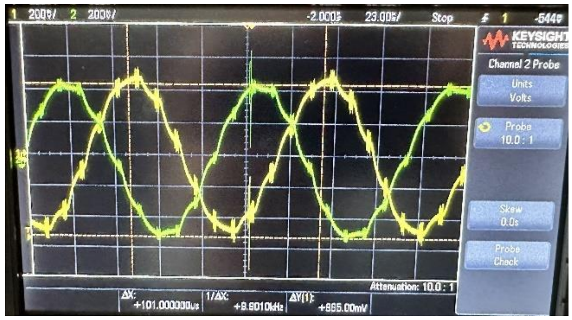

Figure 3.2 Modulated Sine and Cosine waves on an oscilloscope

Now the IQ outputs of the composite circuit (in figure 3.1) were attached to the IQ inputs of the RF signal generator respectively and settings of the frequency at 27.1 MHz and power output were set at -30 dBm. With the IQ inputs then turned on and RF Output also turned on we saw the spectrum analyzer showed a single-sided (upper sideband) modulation with two spikes of 27.0905 MHz on the left side and 27.1105 MHz on the right side giving the spectrum analyzer span as shown in Figure 3.3 (Left). Upon Reversing the IQ inputs of the RF generator, we saw the spectrum being flipped.

Figure 3.3 Spectrum analysis of the modulated signal in Figure 3.2 with IQ out to IQ in connections (Left) and IQ out to QI in (Right)

Having only the I input connected (Q detached) we saw a double-sided modulation which showed both the upper sideband (27)and the low sideband (27.0908 MHz) become of the same magnitude on both sides.

Moving to design streaming of symbols without filtering, we started by designing arrays for streams of the data bits for transmission for each modulation technique which was modeled as shown in the extract from the code in Figure 3.4 where variable I_GAIN and Q_GAIN are assigned data bits ordered by being multiplied by a constant for ordering them for each modulation technique.

```
int32_t BPSK_I[2] = {I_GAIN, -I_GAIN};
int32_t BPSK_Q[2] = {0, 0};

int32_t QPSK_I[2] = {I_GAIN, -I_GAIN};
int32_t QPSK_Q[2] = {Q_GAIN, -Q_GAIN};

int32_t PSK8_I[8] = {I_GAIN*1.00, I_GAIN*0.71, -I_GAIN*0.71, I_GAIN*0.00,
                     I_GAIN*0.71, -I_GAIN*0.00, -I_GAIN*1.00, -I_GAIN*0.71};
int32_t PSK8_Q[8] = {Q_GAIN*0.00, Q_GAIN*0.71, Q_GAIN*0.71, Q_GAIN*1.00,
                     -Q_GAIN*0.71, -Q_GAIN*1.00, -Q_GAIN*0.00, -Q_GAIN*0.71};

int32_t QUAM16_I[4] = {-I_GAIN*1.00, -I_GAIN*0.33, I_GAIN*1.00, I_GAIN*0.33};
int32_t QUAM16_Q[4] = {-Q_GAIN*1.00, -Q_GAIN*0.33, Q_GAIN*1.00, Q_GAIN*0.33};

int32_t QUAM64_I[8] = {-I_GAIN*1.00, -I_GAIN*0.71, -I_GAIN*0.14, -I_GAIN*0.43,
                       I_GAIN*1.00, I_GAIN*0.71, I_GAIN*0.14, I_GAIN*0.43};
int32_t QUAM64_Q[8] = {-Q_GAIN*1.00, -Q_GAIN*0.71, -Q_GAIN*0.14, -Q_GAIN*0.43,
                       Q_GAIN*1.00, Q_GAIN*0.71, Q_GAIN*0.14, Q_GAIN*0.43};
```

Figure 3.4 Modulation Guide arrays

Using this, we set up command line functions that can modulate the selected modulation technique and arrange the symbols for the oscilloscope XY mode which were as shown in Figure 3.5.

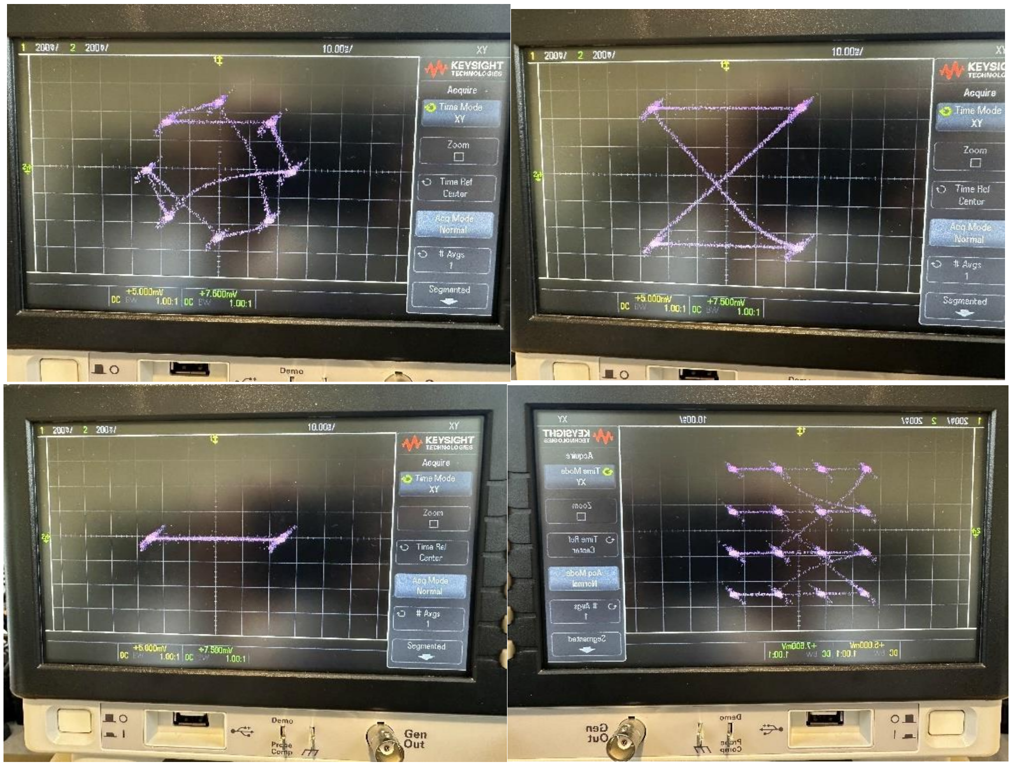

Figure 3.5 Unfiltered Modulated constellations (8PSK top left)(BPSK bottom left)(QPSK top right)(16QAM bottom right)

As shown, the 4 needed unfiltered modulation techniques showed appropriate constellation diagrams. After verifying that proper constellations were made on the oscilloscope, we set it up on FFT mode and received the following plots as shown in figure 3.6

Figure 3.6 FFT of the Unfiltered Modulated signals (BPSK, QPSK, 8PSK, and 16 QAM respectively from left to right)

The FFT of these modulation techniques showed us the frequency spectrum of the modulated signal and the bandwidth of the signal at the baseband as a function of the symbol rate observed from the FFT plot. We observed that the FFT plot showing the signal's frequency content is centered at the carrier frequency, and its bandwidth will be depending on the modulation scheme and its respective symbol rate. We saw a wider bandwidth of the signal with a higher symbol rate which was 16QAM. Observably, the FFT plot also contained the presence of unwanted frequency components which we suspected were noise from the DAC operations and interference from wires.

We then connected the IQ outputs from our circuit to the IQ inputs of the RF signal generator with the defined settings of frequency at 27.1 MHz and power output at -30 dBm with the RF output sent to the spectrum analyzer to see the RF signal's bandwidth as shown in Figure 3.7.

Figure 3.6 Spectrum analysis of the Unfiltered Modulated signals from the RF generator (BPSK, QPSK, 8PSK, and 16 QAM respectively from left to right)

The spectrum analyzer displayed a plot showing the amplitude of the signal on the y-axis and the frequency on the x-axis. This plot showed us the spectral efficiency and the bandwidth occupancy of each modulation technique. By analyzing the plot, we could determine the optimal modulation technique for a particular application based on the desired data rate and available bandwidth. For the figures from the spectrum analyzer, we saw that all the modulations had a center of 27.1 MHz and thus their bandwidths from our measurement were as follows:

BPSK: 27.109 MHz
QPSK: 36.013 MHz
8PSK: 35.931 MHz
16QAM: 32.201 MHz

These values were measured by using the markers on the spectrum analyzer with a lot of noise, so their precision and accuracy were very questionable however these values above were averaged to attain at least precision.

The part where we needed to repeat these measurements after filtering the modulations was uncompleted for our case due to the convolution not being properly creating the arrays, we could write on the DAC but with speculation, we deduced that from filtering the modulated constellations will be more spread out so if they are attenuated or subject to noise the receiving end still may have an idea of the bits being written. This may also bring more unwanted frequencies in the spectrum plot and reduce the bandwidth by improving the spectral efficiency. Therefore, by speculation, an RRC filter could significantly reduce the bandwidth of each modulation technique and improve spectral efficiency while maintaining the desired signal quality for transmission.

Section 4: Conclusion and References

In this lab, we implemented four different digital modulation techniques. The implemented modulation techniques such as Binary Phase Shift Keying (BPSK), Quadrature Phase Shift Keying (QPSK), 8-Phase Shift Keying (8PSK), and 16-Quadrature Amplitude Modulation (16QAM).

These modulated signals were generated using the TM4C123GXL board attached to the dual channel SPI DAC and the operational amplifier (specified in Section 1 and elaborated in Section 3) and transmitted over the RF Signal Generator Modulating over the external IQ channel. This was a way of implementing software-defined radio where we implemented Look Up Tables (LUTs) and modulations based on our Lookup tables for the DAC to write onto the channels (I and Q) of the dual-channel DAC.

We then moved on to observing the modulated signals and their characteristics using an oscilloscope in the FFT mode and XY Mode to see the bandwidth and constellations respectively and compared them with the ideal constellation diagrams of the techniques we attempted to implement.

Through the analysis of the modulated signals, we observed that the higher value of the modulation we used, we had the greater the data rate to be transmitted. This was also the more susceptible the signal is to noise due to fast DAC writes. Where we had to tune the time base of the oscilloscope to get the diagrams, we presented in the Section above. We also attempted to implement RRC filtration, but It is to note that for our hypothesis yet, we were unable to implement properly filtered outputs due to an error in our convolution function thus filtered constellations and their spectrum and FFT plots have been withdrawn from this report.

Additionally, in this lab report, we observed from the Oscilloscope constellations compared with the FFT plots, we saw that QPSK and 8PSK exhibit better spectral efficiency than BPSK due to their ability to transmit more bits per symbol In contrast to 16QAM which was observed to have the highest spectral efficiency among the modulations we implemented with the ability to transmit up to 4 bits per symbol leading the rest as shown in table 4.1.

In speculation, we also found that Constellations with a higher number of points are generally more susceptible to noise. In this lab, the BPSK and QPSK constellations have two and four points respectively, while the 8PSK and 16QAM constellations have 8 and 16 respectively. Therefore, 8PSK and 16QAM constellations are more prone to noise compared to BPSK and QPSK constellations. Overall, this lab provided a comprehensive understanding of digital modulation techniques and designed the discussed modulations in class in real-time for embedded hardware.

Modulation	**Transferable Bits (at an instant)**	**Spectral Efficiency**	**Points in the Constellation diagram**
BPSK	1 Bit	1 Bit/s/Hz	2 Points
QPSK	2 Bits	2 Bits/s/Hz	4 Points
8PSK	3 Bits	3 Bits/s/Hz	8 Points
16 QAM	4 bits	4 Bits/s/Hz	16 Points

Table 4.1 Spectral Efficiency of Modulations used.